AUT Journal of Electrical Engineering
10.22060/eej.2025.23570.5625

Advancing massive MIMO mm-Wave Channel Estimation by Coherence-Optimized Measurement Matrices

Meysam Raees Danaee[1]

[1]Assistant professor, Department of Electrical Engineering, IHCU, Theran, Iran,
email: mraeesdanaee@ihu.ac.ir

Abstract:

In the realm of millimeter-wave communications, despite their promise of high data rates and expansive bandwidths, channel estimation encounters formidable challenges due to conspicuous path loss and the limited multipath components. This paper presents an innovative method that leverages the inherent sparsity of millimeter-wave channels by operating within the two-dimensional transformed domain, this approach treats the channel as a sparse image representation. We advance the accuracy of sparse equivalent vectorized channel recovery by optimizing the measurement matrix. The proposed optimization method significantly reduces the requisite measurements and accelerates the estimation process and minimizes the mean squared error between the true and estimated channel matrices. Through comprehensive simulations, we evaluate our method against two scenarios: one where the compression rate is zero, and the sparse channel matrix recovery relies on the number of observations equating the number of channel matrix elements, and another where the compression rate is non-zero, but the measurement matrix remains unoptimized and randomly selected. Results demonstrate that our method outperforms the latter scenario and achieves accuracy comparable to the former, with significantly reduced computational overhead and accelerated computation speed.

Keywords:

mmWave channel estimation, measurement matrix optimization, sparse channel matrix

AUT Journal of Electrical Engineering
10.22060/eej.2025.23570.5625

1. Introduction

With the advent of fifth and sixth generation wireless communication networks, improving coverage range and enhancing service quality will become essential requirements for the advancement of wireless communications. Even though many systems are operating near their Shannon limit, the fifth generation (5G) still demands significantly higher data rates, approximately 100 to 1000 times greater than previous generations. Researchers have identified three strategies to achieve several orders of magnitude throughput gain: firstly, increasing the density of deployed devices compared to current levels; secondly, utilizing new bandwidths, particularly those in the Millimeter-wave spectrum; and thirdly, deploying a wide array of antennas (massive MIMO) to leverage spatial dimensions for higher data rates. Millimeter-wave (mmWave) communications offer significant advantages for these future wireless communication networks, such as high data rates, large bandwidths, massive antenna arrays, and reduced interference[1]. However, mmWave communications also pose several challenges, such as high path loss, the limited number of multipath components leading to channel sparsity in the angular domain, hardware complexity, and beam alignment[2]. These challenges make estimating the mmWave channel in such a high-frequency band a difficult task.

Various observations have shown that the multipath waves of the received signal in a massive MIMO mm-wave link are distributed into several dominant clusters, exhibiting sparse behavior[3, 4]. Typically, three to four scattering clusters can be observed in urban environments, predominantly in non-line-of-sight (NLOS) conditions. Traditional channel estimation methods are not suitable for such sparse conditions due to the large channel dimensions and the often negligible received components. A common approach for estimating and recovering the limited non-zero elements is utilizing compressive sensing (CS) techniques, which represent the channel with significantly fewer samples than required by the Shannon-Nyquist theorem. Significant research efforts have been dedicated to this area.

There are numerous papers focused on the recovery of sparse signals. Here, we will only address those specifically aimed at channel estimation for massive MIMO mm-wave systems. Orthogonal matching pursuit (OMP) is a greedy algorithm used as CoSaMP in [5] for channel estimation. Additionally, multi-grid OMP (MG-OMP) is proposed in [6] as a modified version of OMP to reduce computational burden and enhance reconstruction adaptability. A generalized version of OMP, known as generalized OMP (GOMP), is presented in[7], which selects more than one index corresponding to the largest correlation in magnitude with the residual in each iteration, thereby accelerating the channel estimation algorithm. A similar idea is explored in [8] with the development of a joint OMP algorithm to perform channel state information reconstruction at the transmitter side, exploiting joint sparsity due to cross-correlation among different user channel matrices. In[9], a traditional OMP algorithm is further developed to propose a new channel estimation scheme named projection-based orthogonal matching pursuit (POMP) to find the minimum number of ADC bits that still offer optimal performance. Greedy methods are also employed in[10-12].

Although basis pursuit (BP) methods and their generalized counterparts, such as least absolute shrinkage and selection operator (LASSO), are rarely implemented in real-time wireless applications due to their high computational complexity, references like [13] have utilized them in channel estimation because they offer much greater accuracy than greedy algorithms. Inspired by the fast iterative shrinkage-thresholding algorithm, [13]presents an accelerated gradient descent algorithm to improve the speed of BP algorithms for channel estimation. To further reduce computational burden, [14]demonstrates that if the angle of arrival (AoA) and angle of departure (AoD) share angular spreads, it is possible to utilize both the sparse nature of the channel and its low-rank structure. In this scenario, [14]proves that the complexity of channel recovery is lower than in cases where only sparsity is considered. In[15], more information is provided about various methods used to estimate the mm-wave channel.

Recently, another category of algorithms based on deep learning networks, such as shown in[16, 17], has been proposed for channel estimation. Instead of modeling the sparsity of the channel, these algorithms

learn channel features in deep layers. These methods excel in addressing highly complex practical issues like limited RF chains, power leakage, and beam squint, which are challenging for CS-based mathematical modeling techniques. However, these approaches require substantial training data and initial computational resources, differing from the current article's focus on reducing computations by leveraging the channel's statistical properties. Bayesian learning, utilizing approximate message passing with unitary transformation (UTAMP-SBL), as described in[18], has demonstrated effective performance with minimal pilot overhead.

The innovation of this paper lies in optimizing the measurement matrix to minimize correlation with the channel dictionary matrix. This idea can be generalized to all CS methods for massive MIMO mm-wave channel estimation, complementing all previously mentioned works. Additionally, as far as the authors are aware, this idea, along with the revised presentation of the channel as a virtual channel, has not yet been applied for massive MIMO mm-wave channel estimation.

The main contribution made in this paper is the optimization of the sensing model's measurement matrix to enhance the quality of this recovery. It is proven that to achieve successful compressed sensing, we must choose a measurement matrix with the least possible coherence with the representing dictionary[19-21]. Recently, there has been significant interest in using optimized matrices to enhance CS-based estimation results[22-24]. Therefore, to reduce the number of required measurements and speed up the estimation process, we propose a new technique in this paper that optimizes the measurement matrix using a gradient descent algorithm to improve the accuracy of sparse equivalent vectorized channel recovery. In other words, the goal is to develop an algorithm for mm-wave channel estimation that maximizes the use of the inherent sparsity of such channels by introducing a coherence-optimized measurement matrix.

For mmWave channel generation using computer simulations, we have used the Saleh-Valenzuela model[1], which is designed for entirely NLOS (urban) paths. In this paper, we first demonstrate that

assuming the channel follows the Saleh-Valenzuela model and considering the limited number of significant paths at the receiver (which is a valid assumption due to the severe attenuation on path loss of millimeter waves), the resulting virtual channel, obtained from the 2D Fourier transform of the mmWave channel, is equivalent to a sparse image. Recovering the locations of the few peaks in this image and finding the corresponding amplitudes is equivalent to estimating the mmWave channel. Consequently, by utilizing compressed sensing algorithms such as a basis pursuit (BP) or a least absolute shrinkage and selection operator (LASSO), we can recover this sparse representation and ultimately estimate the mmWave channel. The notations used in the paper are presented in Table 1.

The paper is organized as follows. The mmWave channel and its virtual channel modeling is described in Section 2. The received observations matrix at the receiver is also modeled in this section. In Section 3, we formulate a CS-based channel estimation method as either a basis pursuit (BP) or a least absolute shrinkage and selection operator (LASSO) problem. Then, we propose a novel method to use an optimized measurement matrix to reduce the number of observations required for the sparse estimation process and to increase the estimation accuracy. Finally, the complexity analysis is presented at the end of Section 3. In Section 4, we evaluate our proposed method under different scenarios and compare it with existing methods. Finally, we conclude the paper in Section 5.

Table 1: Notations Used in the Paper

Symbol	Description
N_t	Number of transmitting antennas
N_r	Number of receiving antennas
$\mathbf{H}$	Channel matrix
$\mathbf{R}$	Received signal matrix
$\boldsymbol{r}$	Vectorized $\mathbf{R}$
$\mathbf{S}$	Pilot signal matrix from the transmitter
$\mathbf{N}$	Complex AWGN noise matrix
$\mathbf{H}_v$	Virtual sparse channel representation

$\mathbf{F}_r$	Fourier transform matrix at the receiver side
$\mathbf{F}_t$	Fourier transform matrix at the transmitter side
α_i	Multipath fading coefficient for the i-th path
θ_i^t, θ_i^r	Angles of departure and arrival for the i-th path at transmitter and receiver
$\boldsymbol{a}(\theta)$	Steering vector at an angle θ
$\boldsymbol{\Phi}$	Measurement matrix used in compressed sensing
$\boldsymbol{\Psi}$	Dictionary matrix
$\mathbf{D}$	Product matrix used in optimization
$\widetilde{\mathbf{D}}$	Column-normalized version of $\mathbf{D}$
λ	Wavelength of carrier signal
γ	Regularization parameter in LASSO
d	Distance between antenna elements
$\boldsymbol{h}_{\mathrm{v}}$	Vectorized virtual channel $\mathbf{H}_{\mathrm{v}}$
K	Number of iterations in gradient descent optimization

2. mmWave channel and virtual channel modeling

For a wireless link with N_t antennas at the transmitter and N_r antennas at the receiver, the accordingly modeled mmWave channel is represented as an $N_r \times N_t$ matrix. The goal of this paper is to propose an appropriate algorithm for estimating this channel matrix by leveraging the inherent properties of the channel. Generally, all its entries may have considerable values, keeping it from being a sparse matrix. However, the mmWave channel can be sparsely represented in another basis (i.e., Fourier).

mmWave communications offer large bandwidths, resulting in a wireless channel that experiences frequency selective multipath fading. However, if we assume the use of OFDM modulation, the mmWave channel can be considered as flat-fading for each of the subcarriers. Given the use of MIMO technology in mmWave communications, for a subcarrier, the channel model is employed assuming omnidirectional

elements of the antenna arrays and a uniform linear array (ULA) configuration on both the transmitter and receiver sides, as follows[1, 25]:

$$\mathbf{H}_{N_r \times N_t} = \sum_{i=1}^{N_{\text{multipath}}} \alpha_i \boldsymbol{a}_r(\theta_i^r)\boldsymbol{a}_t(\theta_i^t)^{\text{H}}, \qquad (1)$$

$$\mathrm{H}_{N_r \times N_t} = \sum_{i=1}^{N_{multipath}} \alpha_i a_r\left(\theta_i^r\right) a_t\left(\theta_i^t\right)^H$$

where the complex coefficient of multipath fading for the ith received path is denoted by α_i. The total number of multipath components received by the receiver is represented by $N_{\text{multipath}}$. The angles of transmission and reception for the signal of the ith received path at the receiver are respectively denoted by θ_i^t and θ_i^r. The steering vectors for these angles at the transmitter and receiver antenna arrays are denoted by $\boldsymbol{a}_t\left(\theta_i^t\right)$ and $\boldsymbol{a}_r(\theta_i^r)$, respectively. The conjugate transpose of $\boldsymbol{a}(\theta)$ is defined to be $\boldsymbol{a}(\theta)^{\text{H}}$.

For a ULA with N elements, $\boldsymbol{a}(\theta)$ is given by:

$$\boldsymbol{a}(\theta) = \tfrac{1}{\sqrt{N}}[1\,, e^{-j\frac{2\pi}{\lambda}d\cos\theta}, \ldots\,, e^{-j\frac{2\pi}{\lambda}d\,(N-1)\cos\theta}]^T, \quad (2)$$

$$a\left(\theta\right) = \frac{1}{\sqrt{N}}\left[1, e^{-j\frac{2\pi}{\lambda}d\cos\theta}, \cdots, e^{-j\frac{2\pi}{\lambda}d\left(N-1\right)\cos\theta}\right]^T$$

10.22060/eej.2025.23570.5625

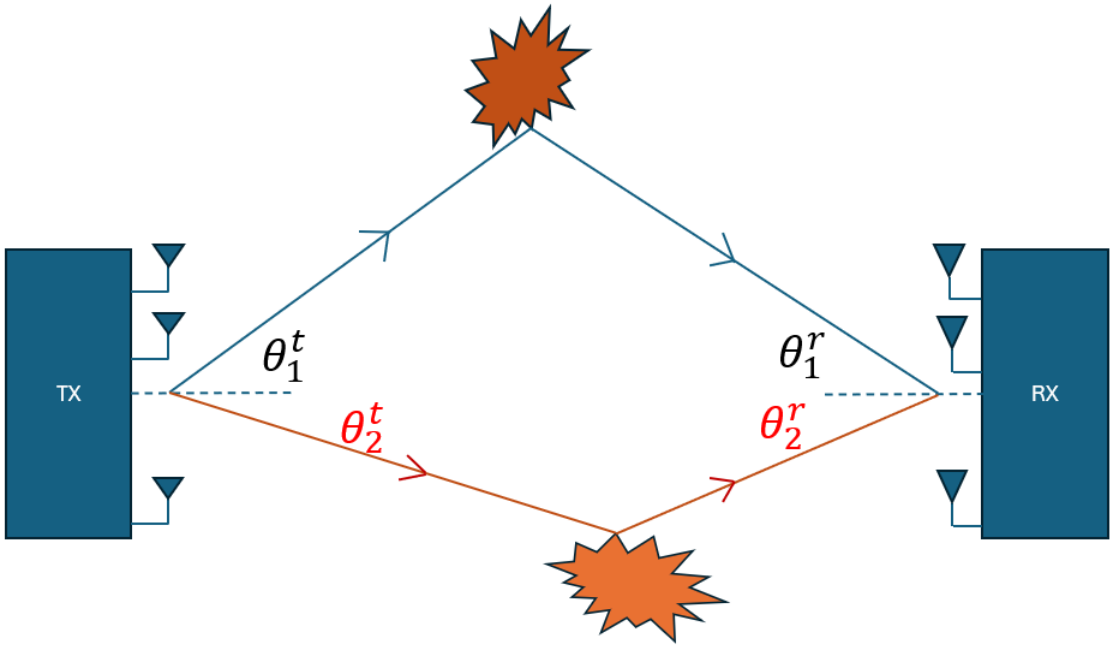

Fig. 1. An illustration of a mm-wave channel environment with two scatterers. In the angular domain, the virtual channel observes only 4 non-zero angles (two at the transmitter and two at the receiver), so it can be represented as sparse. It also considers only 2D wave penetration.

where N represents the number of antenna elements in the array (here, we denote the number of antenna elements for the transmitter and receiver as N_t and N_r, respectively), λ corresponds to the wavelength of the carrier signal, and d is the distance between two adjacent elements in the ULA.

In mmWave communications, the significant path losses result in a very limited number of multipath components being received at the receiver, leading to a sparse representation of the channel in the angular domain. This means $N_{\text{multipath}}$, which denotes the number of multipath components, is a small number. As most reflections are severely attenuated before reaching the destination, the channel can be effectively modeled as sparse in the angular domain, which is also referred to as the virtual channel[13]. This characteristic of mmWave channels necessitates a channel estimation approach that accounts for the inherent sparsity to accurately capture the channel's properties.

10.22060/eej.2025.23570.5625

In Fig. 1, a mm-wave channel environment with two scatterers is illustrated. It is assumed that there is no line-of-sight (LOS) and, due to the severe attenuation of millimeter waves, paths resulting from two consecutive scatterers are generally neglected due to significant weakening. The number of received angles at the receiver will also be limited.

For each subcarrier, the transmitter sends a set of pilot signals N_t times from the transmitter's antenna array with N_t elements through the mmWave channel. These signals form a complex unitary matrix denoted as $\mathbf{S} \in \mathbb{C}^{N_t \times N_t}, \mathbf{S}\mathbf{S}^{\mathrm{H}} = \mathbf{I}_{N_t}$. The effect of the channel $\mathbf{H} \in \mathbb{C}^{N_r \times N_t}$, along with complex AWGN noise $\mathbf{N} \in \mathbb{C}^{N_r \times N_t}$ at the receiver, produces the received matrix $\mathbf{R} \in \mathbb{C}^{N_r \times N_t}$, which is given by the following relationship:

$$\mathbf{R} = \mathbf{H}\mathbf{S} + \mathbf{N}. \quad (3)$$

R=HS+N

The virtual channel, also known as the sparse channel in the angular domain, is represented by $\mathbf{H}_{\mathrm{v}}$ and is obtained by applying a two-dimensional discrete Fourier transform (2D DFT) to the channel matrix $\mathbf{H}$ defined in Eq. (1). To perform a 2D DFT on a matrix $\mathbf{H}$ of size N_r by N_t, we multiply it by two square Fourier matrices $\mathbf{F}_r$ of size $N_r \times N_r$ and $\mathbf{F}_t$ of size $N_t \times N_t$. The result is given by $\mathbf{H}_{\mathrm{v}} = \mathbf{F}_r \mathbf{H} \mathbf{F}_t$. The Fourier matrices $\mathbf{F}_r$ and $\mathbf{F}_t$ are complex matrices whose elements are given by $\mathbf{F}_r[k,l] = exp(-j2\pi\, kl/N_r)$ and $\mathbf{F}_t[k,l] = exp(-j2\pi\, kl/N_t)$, where k and l are the row and column indices, respectively.

On the other hand, the channel matrix $\mathbf{H}$ itself, in terms of the virtual channel representation $\mathbf{H}_{\mathrm{v}}$, is obtained by computing the inverse DFT (IDFT) as follows:

$$\mathbf{H} = \frac{\mathbf{F}_r^{\mathrm{H}}}{N_r} \mathbf{H}_{\mathrm{v}} \frac{\mathbf{F}_t^{\mathrm{H}}}{N_t}. \quad (4)$$

$$\mathrm{H}=\frac{F_r^H}{N_r} H_v \frac{F_t^H}{N_t}$$

10.22060/eej.2025.23570.5625

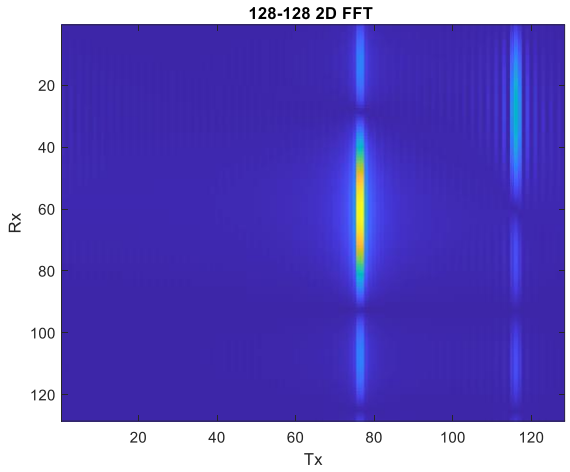

Fig. 2. An illustration sparse image representation of the virtual channel matrix created by padding virtual channel matrix with trailing zeros to form an 128-by-128 matrix and then computing its two-dimensional Fourier transform for only two scatters with $\theta_1^t = 13, \theta_2^t = 95, \theta_1^r = 5, \theta_2^r = 45$, and $\lambda = 2.5d$, $N_r = 4$, $N_t = 64$.

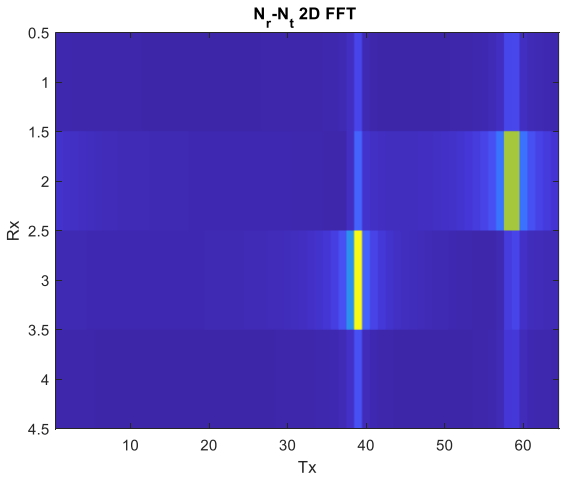

Fig. 3. An illustration sparse image representation of the virtual channel matrix created by padding virtual channel matrix with trailing zeros to form an N_r-by-N_t matrix and then computing its two-dimensional Fourier transform will parameter setting similar of Fig. 2.

As mentioned in the abstract, this method represents the virtual channel as a sparse image. In Fig. 2 and Fig. 3, the sparse images of the virtual channel are depicted for two different strategy of zero padding in Fig. 2 and no zero padding in Fig. 3. To avoid ambiguities in the spatial sampling of the array, λ is set to

2.5d. According to Fig. 2 and Fig.3, each angle at the transmitter (receiver) corresponds to a peak on the vertical (horizontal) axis of the sparse image representation of the virtual channel matrix. This matrix is the Fourier transform of the millimeter-wave channel, calculated according to Eq. (4).

By substituting Eq. (4) into Eq. (3), the model for the received observations matrix **R** in terms of the sparse virtual channel matrix $\mathbf{H}_{\mathrm{v}}$ is expressed as:

$$\mathbf{R} = \frac{\mathbf{F}_r^{\mathrm{H}}}{N_r} \mathbf{H}_{\mathrm{v}} \frac{\mathbf{F}_t^{\mathrm{H}}}{N_t} \mathbf{S} + \mathbf{N}. \qquad (5)$$

$$\mathrm{R} = \frac{F_r^H}{N_r} H_v \frac{F_t^H}{N_t} \mathrm{S+N}$$

3. CS-Based Channel Estimation

Here, we aim to improve and innovate the use of compressed sensing algorithms to enhance channel estimation accuracy with a fixed number of observations. Generally, in a mmWave channel, OFDM modulation is used to overcome frequency-selective fading, ensuring that each of its subcarriers experiences flat fading.

3-1- Problem formulation

The concept of using compressive sensing (CS) in channel estimation is to first estimate the virtual channel matrix $\mathbf{H}_{\mathrm{v}}$.

As explained, in mmWave channels, due to high signal absorption in the environment, only a few paths remain that can reach the receiver. Therefore, the number of received angles (and correspondingly, the number of transmitted angles) in the channel is small. This means that the channel $\mathbf{H}_{\mathrm{v}}$ is sparse, and it is not necessary to estimate all its $N_t N_r$ components. Moreover, to recover the non-zero values, the number of measurements (the number of solvable equations) does not need to equal the number of entries of $\mathbf{H}_{\mathrm{v}}$. It is possible to uniquely recover $\mathbf{H}_{\mathrm{v}}$ with fewer measurements than the number of unknowns $N_t N_r$.

10.22060/eej.2025.23570.5625

However, since the location of the non-zero elements in $\mathbf{H}_{\mathrm{v}}$ is not known, the number of observations cannot be too low for the recovery of $\mathbf{H}_{\mathrm{v}}$ to be possible. To find the relationships between the degree of sparsity and the number of measurements required for a successful sparse vector recovery, please refer to[26].

To exploit the sparsity of the mmWave channel in the angular domain, we use the sparse equivalent vectorized channel model $\boldsymbol{h}_{\mathrm{v}} = \mathrm{vec}(\mathbf{H}_{\mathrm{v}})$. We can also use the Kronecker product to vectorize the 2D DFT in Eq. (5) as:

$$\boldsymbol{r} = (\mathbf{F}_t^{\mathrm{H}}\mathbf{S}/N_t \otimes \mathbf{F}_r^{\mathrm{H}}/N_r)\boldsymbol{h}_{\mathrm{v}} + \boldsymbol{n}. \quad (6)$$

$$r = \left(F_t^H S / N_t \otimes F_r^H / N_r\right) h_v + n$$

where $\boldsymbol{r} = \mathrm{vec}(\mathbf{R})$, $\boldsymbol{n} = \mathrm{vec}(\mathbf{N})$ and $\otimes$ denotes the Kronecker product. In the literature of compressive sensing, if we denote $\left(\mathbf{F}_t^{\mathrm{H}}\mathbf{S}/N_t \otimes \mathbf{F}_r^{\mathrm{H}}/N_r\right)$ as $\boldsymbol{\Psi} \in \mathbb{C}^{N_r N_t \times N_r N_t}$, then $\boldsymbol{\Psi}$ is referred to as the "representing dictionary matrix", so

$$\boldsymbol{r} = \boldsymbol{\Psi}\boldsymbol{h}_{\mathrm{v}} + \boldsymbol{n}. \quad (7)$$

$$r = \Psi h_v + n$$

Based on the principles of compressive sensing, we aim to identify N_c measurements, each being a linear function of the elements of the vector $\boldsymbol{\Psi}\boldsymbol{h}_{\mathrm{v}}$ to recover $\boldsymbol{h}_{\mathrm{v}}$. The number of measurements N_c should be less than, and preferably much less than, $N_r N_t$. Therefore, we multiply the vector $\boldsymbol{\Psi}\boldsymbol{h}_{\mathrm{v}}$ from the left by the matrix $\boldsymbol{\Phi} \in \mathbb{R}^{N_c \times N_t N_r}$, which we refer to as the "measurement matrix", to reduce the number of measurements used for estimating $\boldsymbol{h}_{\mathrm{v}}$ from $N_r N_t$ to N_c.

$$\boldsymbol{r}_c = \boldsymbol{\Phi}\boldsymbol{\Psi}\boldsymbol{h}_{\mathrm{v}} + \boldsymbol{\Phi}\boldsymbol{n}. \quad (8)$$

$$r_c = \Phi\Psi h_v + \Phi n$$

where$\boldsymbol{r}_c$ denotes the reduced size (compressed) measurements. In general, the entries of the observation matrix $\boldsymbol{\Phi}$ are generated completely at random, following a distribution such as the standard Gaussian distribution[27].

The basis pursuit (BP) relaxed with l_1 norm minimization problem, [26], and the least absolute shrinkage and selection operator (LASSO), [28], are both methods used in the context of sparse recovery.

The BP relaxed with l_1 norm minimization problem focuses solely on the minimization of the l_1 norm of the coefficient vector where the goal is to recover a sparse signal from a small number of linear measurements which is subject to constraints that ensure the solution is consistent with the observed data. This problem can be represented as:

$$\begin{aligned} \boldsymbol{h}_{\mathrm{v}}^{*} &= \min\|\boldsymbol{h}_{\mathrm{v}}\|_1 \\ \text{subject to } \boldsymbol{r}_c &= \boldsymbol{\Phi}\boldsymbol{\Psi}\boldsymbol{h}_{\mathrm{v}} \\ h^{*}_{v} &= \min\left\|h_v\right\|_1 \\ s.t. \quad r_c &= \Phi\Psi h_v \end{aligned} \tag{9}$$

The LASSO is a regression method that involves adding a l_1 norm penalty to the sum squared error (SSE) loss function. The objective function for LASSO is given by:

$$\boldsymbol{h}_{\mathrm{v}}^{*} = \arg\min_{\boldsymbol{h}_{\mathbf{v}}}(\|\boldsymbol{r}_c - \boldsymbol{\Phi}\boldsymbol{\Psi}\boldsymbol{h}_{\mathrm{v}}\|_2^2 + \gamma\|\boldsymbol{h}_{\mathrm{v}}\|_1) \tag{10}$$

$$h^{*}_{v} = \arg\min_{h_v}\left(\left\|r_c - \Phi\Psi h_v\right\|_2^2 + \gamma\left\|h_v\right\|_1\right)$$

γ is the regularization parameter that controls the strength of the penalty. The LASSO method aims to both minimize the residual sum of squares and enforce sparsity in the coefficients. The regularization parameter γ that needs to be chosen, which balances the trade-off between the loss function (noise reduction) and the penalty term (sparse recovery).

3-2- Measurement Matrix Design and Optimization

Numerous studies have established that a low mutual coherence between the measurement matrix and the representing dictionary matrix is essential for the successful application of compressive sensing[29], [20],[30]. Consequently, it is advantageous to design measurement matrices that exhibit minimal coherence with the representing dictionary to enhance the efficacy of compressive sensing in mmWave channel estimation.

In our pursuit of optimal mmWave channel estimation, we must select a measurement matrix, $\mathbf{\Phi}$, that exhibits the lowest possible coherence with the sparsity basis (or representing dictionary), $\mathbf{\Psi}$. This implies that if we define $\mathbf{D} = \mathbf{\Phi\Psi}$, the columns of $\mathbf{D}$ should have minimal correlation. Consequently, the ideal scenario is that the Gramian matrix of the column-normalized version of $\mathbf{D}$, denoted as $\widetilde{\mathbf{D}}$, is equal to the identity matrix $\mathbf{I}_{N_t N_r}$.

The Gramian matrix of $\widetilde{\mathbf{D}}$, is given by $\widetilde{\mathbf{D}}^{\mathrm{H}}\widetilde{\mathbf{D}}$. Note that $\widetilde{\mathbf{D}}^{\mathrm{H}}\widetilde{\mathbf{D}}$ is not full-rank because it has $N_t N_r - N_c$ eigenvalues equal to zero. It follows that $\widetilde{\mathbf{D}}^{\mathrm{H}}\widetilde{\mathbf{D}}$ cannot be equal to $\mathbf{I}_{N_t N_r}$, but we can select $\mathbf{\Phi}$ such that for a given $\mathbf{\Psi}$, the Gramian matrix of $\widetilde{\mathbf{D}}$ is as close to the identity matrix $\mathbf{I}_{N_t N_r}$ as possible. One approach to achieve this objective is to solve the following optimization problem:

$$\widetilde{\mathbf{D}}^{*} = \arg\min_{\widetilde{\mathbf{D}}} \left(\left\| \widetilde{\mathbf{D}}^{\mathrm{H}}\widetilde{\mathbf{D}} - \mathbf{I}_{N_t N_r} \right\|_F^2 \right), \qquad (11)$$

$$\mathrm{D}^{*} = \arg\min_{\mathrm{D}} \left(\left\| \mathrm{D}^{\mathrm{H}}\mathrm{D} - \mathrm{I}_{N_t N_r} \right\|_F^2 \right)$$

where $\|\cdot\|_F$ denotes the Frobenius norm. In this paper we propose to employ a numerical method- i.e., gradient descent, to solve Eq. (11) iteratively. A feasible initial value for $\widetilde{\mathbf{D}}$ can be obtained by generating$\mathbf{\Phi}$ from the standard multivariate normal distribution and then multiplying it with $\mathbf{\Psi}$. Then, in K successive iterations, the value of $\widetilde{\mathbf{D}}$ can be updated according to the following formula:

$$\widetilde{\mathbf{D}}_{n+1} = \widetilde{\mathbf{D}}_n - \alpha \nabla_{\widetilde{\mathbf{D}}} \left(\left\| \widetilde{\mathbf{D}}_n{}^{\mathrm{H}}\widetilde{\mathbf{D}}_n - \mathbf{I}_{N_t N_r} \right\|_F^2 \right), \qquad (12)$$

10.22060/eej.2025.23570.5625

$$\mathrm{D}_{n+1} = \mathrm{D}_n - \alpha \nabla_{\mathrm{D}} \left(\left\| \mathrm{D}^{\mathrm{H}}\mathrm{D} - \mathrm{I}_{N_t N_r} \right\|_F^2 \right)$$

where α is the step size in the gradient descent method and for the scaler function $G(\cdot)$, $\nabla_{\widetilde{\mathbf{D}}} G(\widetilde{\mathbf{D}}_n)$ is the gradient of $G(\cdot)$ with respect of $\widetilde{\mathbf{D}}$ at $\widetilde{\mathbf{D}}_n$. The final updated $\widetilde{\mathbf{D}}_n$ is chosen to be the solution of Eq. (11), denoted as $\widetilde{\mathbf{D}}^*$. The gradient of $\| \widetilde{\mathbf{D}}^{\mathrm{H}}\widetilde{\mathbf{D}} - \mathbf{I}_{N_t N_r} \|_F^2$ with respect to $\widetilde{\mathbf{D}}$ is given by the following formula[31]:

$$\nabla_{\widetilde{\mathbf{D}}} \left(\| \widetilde{\mathbf{D}}^{\mathrm{H}}\widetilde{\mathbf{D}} - \mathbf{I}_{N_t N_r} \|_F^2 \right) = 4\widetilde{\mathbf{D}}\left(\widetilde{\mathbf{D}}^{\mathrm{H}}\widetilde{\mathbf{D}} - \mathbf{I}_{N_t N_r}\right) \qquad (13)$$

$$\nabla_{\mathrm{D}} \left(\left\| \mathrm{D}^{\mathrm{H}}\mathrm{D} - \mathrm{I}_{N_t N_r} \right\|_F^2 \right) = 4\mathrm{D}\left(\mathrm{D}^{\mathrm{H}}\mathrm{D} - \mathrm{I}_{N_t N_r} \right)$$

By plugging Eq. (13) into Eq. (12), we complete the solution of the optimization problem in Eq. (11). Finally, we obtain the measurement matrix $\boldsymbol{\Phi}$ as $\widetilde{\mathbf{D}}^*\boldsymbol{\Psi}^{-1}$. We can then apply it to the received observation $\boldsymbol{r}$ in Eq. (7) to obtain reduced size $\boldsymbol{r}_c$ in Eq. (8) and solve either the relaxed basis pursuit problem in Eq. (9) or the LASSO in Eq. (10) to estimate the virtual channel coefficients $\boldsymbol{h}_{\mathrm{v}}^*$. The pseudo code for the proposed massive MIMO mm-Wave channel estimation methods with non-optimized $\boldsymbol{\Phi}$ and with optimized $\boldsymbol{\Phi}$ are presented in Algorithm 1.

10.22060/eej.2025.23570.5625

Algorithm 1: Pseudo code for the proposed massive MIMO mm-Wave Channel Estimation methods

1. For N_t iterations, transmit the pilot vector $\boldsymbol{s}_i \in \mathbb{C}^{N_t \times 1}$ from the transmitter antennas such that $[\boldsymbol{s}_1, \cdots, \boldsymbol{s}_i, \cdots, \boldsymbol{s}_{N_t}]$ forms the unitary matrix $\mathbf{S}$.
2. Since the matrix $\mathbf{S}$ is known at the receiver, compute the representing dictionary $\boldsymbol{\Psi}$ according to $\left(\mathbf{F}_t^{\mathrm{H}}\mathbf{S}/N_t \otimes \mathbf{F}_r^{\mathrm{H}}/N_r\right)$.
3. Upon receiving the matrix $\mathbf{R}$ at the receiver, vectorize it to form $\boldsymbol{r}$, then compute $\boldsymbol{r}_c$ using Eq. (8).
4. If the problem is to be solved with optimized $\boldsymbol{\Phi}$, compute the matrix $\widetilde{\mathbf{D}}^*$ according to equation Eq. (12) recursively, and then obtain the measurement matrix $\boldsymbol{\Phi}$ as $\widetilde{\mathbf{D}}^*\boldsymbol{\Psi}^{-1}$.
5. Calculate the recovered vector $\boldsymbol{h}_{\mathrm{v}}^*$ by solving the optimization problem BP in equation Eq. (9) or the LASSO optimization problem (assuming an appropriate γ is chosen) in equation Eq. (10).
6. Obtain $\mathbf{H}_{\mathrm{v}}^*$, the matrix equivalent of the vector $\boldsymbol{h}_{\mathrm{v}}^*$, and finally estimate the mmWave channel $\mathbf{H}^*$ using equation Eq. (4).

3-3- Complexity analysis

The gradient computation involves matrix multiplications and subtractions. As $\widetilde{\mathbf{D}}$ is an $N_c \times (N_t N_r)$ matrix, the complexity of computing $\widetilde{\mathbf{D}}^{\mathrm{H}}\widetilde{\mathbf{D}}$ is $\mathcal{O}(N_c(N_t N_r)^2)$, and the complexity of computing the gradient is also $\mathcal{O}(N_c(N_t N_r)^2)$. The gradient descent update step involves matrix addition and subtraction, which is $\mathcal{O}(N_c N_t N_r)$. So, the total complexity per iteration is dominated by the gradient computation, which is $\mathcal{O}(N_c(N_t N_r)^2)$. The overall complexity also depends on the number of iterations required for the algorithm to converge, which can vary based on the learning rate and the specific properties of the objective function.

The computed $\widetilde{\mathbf{D}}$ is then utilized by either BP or LASSO. Basis Pursuit is typically solved using linear programming (LP) techniques such as the interior point method, where its complexity is $\mathcal{O}((N_c + N_t N_r)^{1.5}(N_t N_r)^2)$. Given $N_t N_r$ is much larger than N_c, the complexity is dominated by $N_t N_r$, leading to $\mathcal{O}((N_t N_r)^{3.5})$. Basis pursuit has a higher complexity and is generally more suitable for smaller problems.

LASSO can be solved using techniques such as coordinate descent. The complexity of solving the LASSO problem using coordinate descent is $\mathcal{O}(N_c N_t N_r \log(\epsilon^{-1}))$, where ϵ is the desired accuracy of the solution. LASSO is typically more efficient for larger problems due to its linear complexity in terms of N_c and $(N_t N_r)$.

It is also insightful to compare the above results with those of SPC[13], a method that will be used as a counterpart algorithm in the simulation section.

The SPC[13] algorithm primarily involves DFT and IDFT of size $N_t \times N_r$ for virtual channel representation. The complexity of each transformation is $\mathcal{O}(N_t N_r \log_2(N_t N_r))$. It also involves iterative steps for the identification of peaks and cancellation of corresponding sinc functions. At each iteration, the algorithm identifies the maximum magnitude element in the $N_t \times N_r$ matrix with complexity $\mathcal{O}(N_t N_r)$. For each detected path, a sinc function is computed and subtracted. The complexity per iteration is $\mathcal{O}(N_t N_r)$. The number of iterations I corresponds to the number of paths to be estimated, so the total iterative complexity becomes $I\mathcal{O}(N_t N_r) = \mathcal{O}(IN_t N_r)$. Finally, the total complexity is computed by adding the contributions as $2\mathcal{O}(N_t N_r \log_2(N_t N_r)) + \mathcal{O}(IN_t N_r)$.

4. Simulation results

We assume that the antennas are arranged in a uniform linear array (ULA) and that the number of antennas at the UE is limited, i.e., $N_r = 4$. For mmWave, we consider the carrier frequency to be 30 GHz, $\lambda = \frac{3e8}{30e9}, d = \lambda/2.5$.

We set $N_t = 64$ as the number of antennas at the BS. All the results are obtained by averaging over 200 independent runs for each scenario. We assume that there are only two multipath components in the channel, i.e., two angles of departure and two angles of arrival. In practice, both the number of paths and the angles are random, but we simplify the channel scenario to focus on the performance of the algorithms. The simulation parameters are presented in Table 2.

Table 2: Simulation Parameters

Symbol	Value	Description
Carrier Frequency	30 GHz	Frequency used in mmWave simulation
Antenna Spacing d	$\lambda/2.5$	Distance between adjacent elements in ULA
Number of Receiver Antennas N_r	4	Number of antennas at the User Equipment (UE)
Number of Transmitter Antennas N_t	64	Number of antennas at the Base Station (BS)
SNR	10 dB	Signal-to-Noise Ratio during simulations
Compression Rate	0%, 20%, 50%, 75%	Rates at which observations are reduced
LASSO Regularization Parameter γ	10	Regularization parameter used in LASSO optimization
Number of Independent Runs	200	Number of simulations per scenario for averaging results
Number of Paths	2	Number of multipath components in the mmWave channel

10.22060/eej.2025.23570.5625

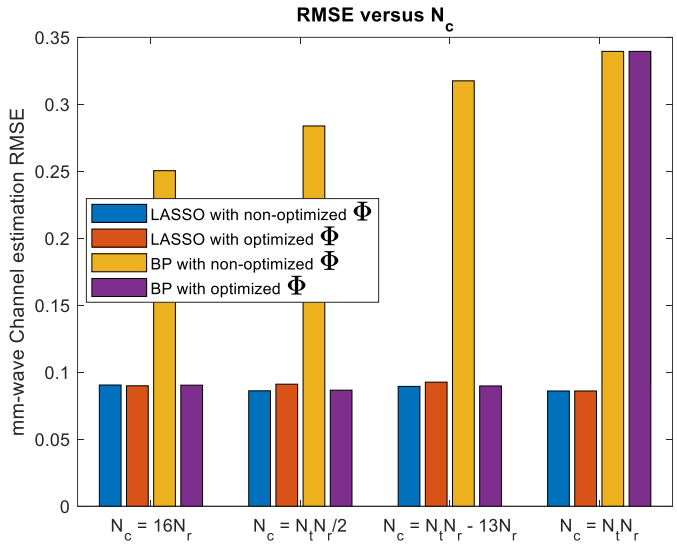

Fig. 4. The effect of compression rate N_c on RMSE of mm-wave channel estimation.

First, we find the appropriate value of γ for solving the LASSO problem for the case where the compression rate is zero. In other words, we assume that the measurement matrix $\mathbf{\Phi}$ is equal to the identity matrix $\mathbf{I}_{N_tN_r}$. The best value for γ was obtained as 10. In the following simulations, we investigate the effect of compressive sensing, or the reduction of observations, by multiplying the measurement matrix $\mathbf{\Phi}$ with the dictionary matrix $\mathbf{\Psi}$ for different values of N_c. We consider the SNR to be 10 dB, and we set N_c to N_tN_r (no reduction of observations and $\mathbf{\Phi} = \mathbf{I}_{N_tN_r}$), $N_tN_r - 13N_r$ (20% reduction of observations), $N_tN_r/2$ (half of the channel matrix elements), and $16N_r$ (16 times the sparsity degree of the channel matrix in the angular domain, which is 4). We perform this analysis for both the LASSO and the BP optimization problems. For each value of N_c and for each optimization problem, we generate the matrix $\mathbf{\Phi}$ in two ways. In the first method, which we call non-optimized, $\mathbf{\Phi}$ is generated from the standard multivariate normal distribution. In the second method, $\mathbf{\Phi}$ is optimized, as explained in Eq. (11) to Eq. (13). The RMSE values of the channel estimation obtained for the mentioned algorithms are shown in Fig. 4 as a function of N_c. An interesting point is that the BP algorithm is much more sensitive to the choice of $\mathbf{\Phi}$ than the LASSO algorithm, and its performance for the non-optimized case is much weaker than the optimized case.

10.22060/eej.2025.23570.5625

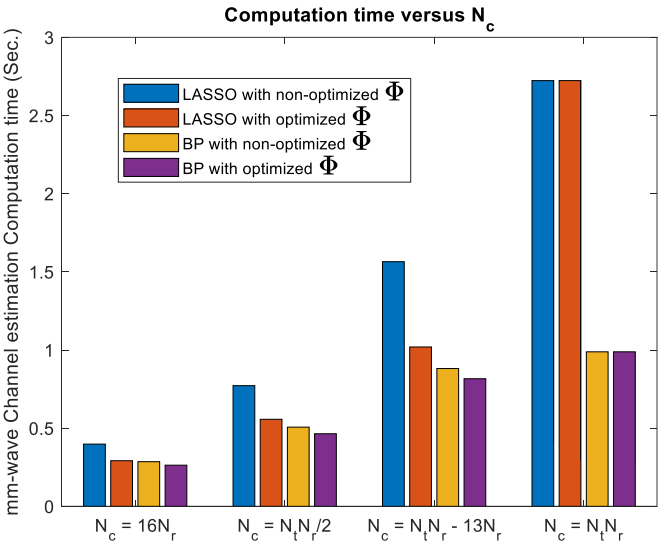

Fig. 5. The effect of compression rate N_c on computation time.

Moreover, for the LASSO algorithm, increasing the compression rate does not cause much performance degradation, but as shown in Fig. 5, the computation speed increases by more than three times when N_c is reduced to $16N_r$ compared to the case where the LASSO algorithm only reduces the observations by 20%.

The average computation time for each solution is plotted in Fig. 5 for all these scenarios. It is natural that the computation time increases as the compression rate decreases, i.e., as N_c increases. Moreover, Fig. 5 indicates that the LASSO method requires more computation time than the BP method. In the last simulation, we observe the effect of SNR changes (from -5 dB to 20 dB) on the performance metric of mmWave channel estimation, i.e., RMSE.

We set N_c to the minimum value from the previous simulation, i.e., $16N_r$, to achieve the maximum computation speed. For each SNR value, we generate the matrix $\mathbf{\Phi}$ in two ways, non-optimized and optimized, for both the LASSO and the BP optimization problems. Along with these simulations, we also plot the RMSE of the channel estimation as a function of SNR for the least square (LS) algorithm and SPC[13]. The results of these simulations are shown in Fig. 6.

10.22060/eej.2025.23570.5625

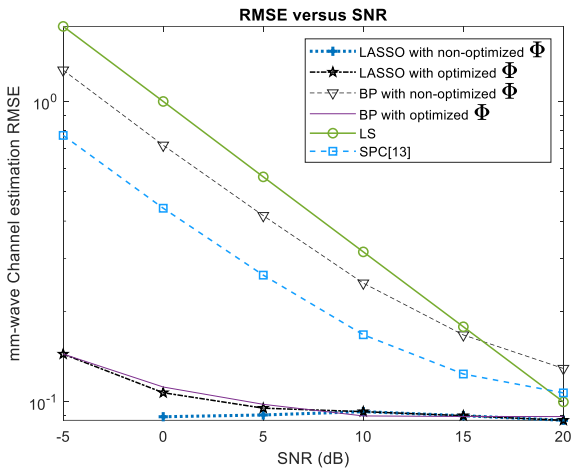

Fig. 6. The effect of SNR on RMSE of mm-wave channel estimation.

As shown in Fig. 6, the performance generally improves as the SNR increases, which is expected. The LS method has the worst performance among all the algorithms, especially at low SNRs. The data presented in Fig. 6 indicates that, despite their lower computational burden and higher speed compared to the our proposed algorithms, the LS and SPC[13] methods exhibit inferior performance in retrieving sparce mm-wave channel.

The BP algorithm performs much better when the matrix $\mathbf{\Phi}$ is optimized than when it is not optimized. In general, due to the regularization term in the objective function of the LASSO problem (which takes into account the noise effect), the LASSO method performs better than the BP method, regardless of whether the matrix $\mathbf{\Phi}$ is optimized or not. However, the BP algorithm also achieves a performance close to the LASSO method, if it uses the matrix $\mathbf{\Phi}$ that is optimized. A surprising point is that for the LASSO problem, using the matrix $\mathbf{\Phi}$ that is not optimized gives a better performance than using the one that is optimized. The authors speculate that perhaps the value of γ used in this method needs to be updated and is not optimal. This is because the value obtained was for the case of no compression, i.e., for $\mathbf{\Phi} = \mathbf{I}_{N_t N_r}$.

Greedy algorithms like OMP are computationally efficient but require prior knowledge of the sparsity level for effective performance. Without this, OMP may either stop prematurely or continue unnecessarily, impacting recovery performance. In contrast, optimization-based methods like basis

pursuit (BP) do not require knowledge of the sparsity level, as they enforce sparsity through l_1-norm minimization. However, BP methods are generally more computationally intensive than greedy algorithms due to the need to solve convex optimization problems.

5. Conclusion

In this paper, we propose a novel method for estimating the mmWave channel by exploiting its inherent sparsity. In this method, we optimize the measurement matrix $\mathbf{\Phi}$ such that it has the lowest coherence with the representing dictionary matrix $\mathbf{\Psi}$. The result of this idea is a significant improvement in the mmWave channel estimation algorithm using the BP method, and a much lower computational complexity than the case where the compression rate is zero, i.e., $\mathbf{\Phi} = \mathbf{I}$. However, this method does not benefit much from using the LASSO algorithm. In general, utilizing sparsity in mmWave channel estimation, whether by using BP or LASSO, leads to higher estimation accuracy than the conventional LS method, which does not use the channel sparsity.

6. References

[1] T.S. Rappaport, Overview of millimeter wave communications for fifth-generation (5G) wireless networks—With a focus on propagation models.
[2] Y. Niu, A survey of millimeter wave communications (mmWave) for 5G: opportunities and challenges.
[3] A. Ghosh, Millimeter-wave enhanced local area systems: A high-data-rate approach for future wireless networks.
[4] S. Sun, Millimeter wave MIMO channel estimation based on adaptive compressed sensing.
[5] W.U. Bajwa, Compressed channel sensing: A new approach to estimating sparse multipath channels.
[6] J. Lee, Exploiting spatial sparsity for estimating channels of hybrid MIMO systems in millimeter wave communications.
[7] J. Wang, Generalized orthogonal matching pursuit.
[8] X. Rao, Distributed compressive CSIT estimation and feedback for FDD multi-user massive MIMO systems.
[9] O. Oyerinde, Compressive sensing-based channel estimation schemes for wideband millimeter wave wireless communication systems.
[10] N. Sadeghi, Channel estimation using block sparse joint orthogonal matching pursuit in massive MIMO systems.
[11] W. Shen, Massive MIMO channel estimation based on block iterative support detection.
[12] Y. Li, Joint Doppler shift and channel estimation for UAV mmWave system with massive ULA.
[13] H. Soleimani, D. De Donno, S. Tomasin, mm-Wave channel estimation with accelerated gradient descent algorithms, EURASIP Journal on Wireless Communications and Networking, 2018(1) (2018) 1-17.

[14] X. Li, Millimeter wave channel estimation via exploiting joint sparse and low-rank structures.
[15] H. Kais, Channel estimation techniques for millimeter-wave communication systems: Achievements and challenges.
[16] J. Gao, Deep learning-based channel estimation for wideband hybrid mmWave massive MIMO.
[17] S. Liu, Sparsity-aware channel estimation for mmWave massive MIMO: A deep CNN-based approach.
[18] S. Hou, Uplink sparse channel estimation for hybrid millimeter wave massive MIMO systems by UTAMP-SBL.
[19] L. Shi, G. Qu, An Improved Reweighted Method for Optimizing the Sensing Matrix of Compressed Sensing, IEEE Access, (2024).
[20] V. Abolghasemi, S. Ferdowsi, B. Makkiabadi, S. Sanei, On optimization of the measurement matrix for compressive sensing, in: 2010 18th European Signal Processing Conferenc, 2010.
[21] R. Jacome, H. Arguello, A. Hernandez-Rojas, P. Goyes-Penafiel, Divergence-based regularization for end-to-end sensing matrix optimization in compressive sampling systems, SIGNAL 2023 Editors, (2023).
[22] H. Liu, C. Song, Z. Li, Z. Liu, L. Ta, A New Method for The Identification of Earthquake-damaged Buildings Using Sentinel-1 Multi-temporal Coherence Optimized by Homogeneous SAR Pixels and Histogram Matching, IEEE Journal of Selected Topics in Applied Earth Observations and Remote Sensing, (2024).
[23] M. HAROON AURANGZEB, F. AKRAM, I. RASHID, A. AHMED, Pilots Optimization and Surface Area Effects on Channel Estimation in RIS Aided MIMO System, Radioengineering, 32(2) (2023).
[24] L. Peng, X. Zhang, G.K.-L. Chan, Fermionic reduced density low-rank matrix completion, noise filtering, and measurement reduction in quantum simulations, Journal of Chemical Theory and Computation, 19(24) (2023) 9151-9160.
[25] Y. Liu, C.-X. Wang, J. Huang, J. Sun, Novel 3-D nonstationary mmWave massive MIMO channel models for 5G high-speed train wireless communications, IEEE Transactions on Vehicular Technology, 68(3) (2018) 2077-2086.
[26] S. Foucart, H. Rauhut, An invitation to compressive sensing, Springer, 2023.
[27] E.J. Candes, J.K. Romberg, T. Tao, Stable signal recovery from incomplete and inaccurate measurements, Communications on Pure and Applied Mathematics: A Journal Issued by the Courant Institute of Mathematical Sciences, 59(8) (2006) 1207-1223.
[28] R. Tibshirani, Regression shrinkage and selection via the lasso, Journal of the Royal Statistical Society Series B: Statistical Methodology, 58(1) (1996) 267-288.
[29] M. Elad, Optimized projections for compressed sensing, IEEE Transactions on Signal Processing, 55(12) (2007) 5695-5702.
[30] B. Kilic, A. Gungor, M. Kalfa, O. Arikan, Adaptive measurement matrix design in direction of arrival estimation, IEEE Transactions on Signal Processing, 70 (2022) 4742-4756.
[31] K.B. Petersen, M.S. Pedersen, The matrix cookbook, 7(15) (2008) 510.